Characterization of Microporous Titanosilicate ETS-10 by Infrared Spectroscopy with Methane as a Probe Molecule for Basic Sites

Madoka Kishima and Tatsuya Okubo*

Department of Chemical System Engineering, The University of Tokyo, 7-3-1 Hongo, Bunkyo-ku, Tokyo 113-8656, Japan

Received: November 10, 2002; In Final Form: May 19, 2003

In situ infrared spectroscopy with probe molecules is a useful technique for the characterization of solid surfaces. The selection of an appropriate probe molecule is critical for this technique. In this study, the usefulness of methane as a probe for basic sites in microporous titanosilicate ETS-10 is demonstrated. With the help of carbon monoxide as a probe for cationic sites, some absorption bands of methane were assigned as methane molecules adsorbed on basic sites. The frequencies of these bands indicated that the strengths of the basic sites of Na-ETS-10 and Cs-ETS-10 are in the same degree with those of MgO, NaY, and CsY. On the basis of the spectroscopic results, the locations of the adsorption sites in the crystal framework are also discussed.

1. Introduction

Characterization of active sites and potential fields on solid surfaces or in the pores of porous materials provides useful information for applications involving catalysis or adsorption. Compared with the methods used for acidic sites, the methods for the characterization of basic sites are not yet well established. In situ infrared spectroscopy with probe molecules is a useful technique for this purpose. This technique is based on the phenomenon that the vibrational frequency of a probe molecule changes in an electric field (the vibrational Stark effect[1]) and it also changes along with the charge transfer caused by chemisorption. The selection of an appropriate probe molecule is critical for this technique, and the requirements for a probe molecule are well summarized in a review by Knözinger.[2] Several probe molecules have been tested and reviewed[2−4] for the characterization of basic sites. Potential probe molecules are, for example, C−H acids such as chloroform, acetylene, and methane, and N−H acids such as pyrrole. Among these probe molecules, methane has the following advantages: low reactivity, small molecular size, and simple molecular structure that gives a simple absorption spectrum. Moreover, methane is advantageous because competitive adsorption with carbon monoxide can partly solve the critical problem of the characterization of basic sites. In other words, whereas the probe molecules mentioned above are adsorbed on the basic sites, they are also sensitive[4−6] to the existing electric fields; an example would be the area proximal to the extraframework cations of zeolites. Carbon monoxide has a smaller intermolecular interaction energy than methane (the Lennard-Jones energy ϵ_{LJ}/k of methane is 148.6 K[7] and that of carbon monoxide is 91.7 K[7]), and it also has a permanent dipole moment, both of which mean that carbon monoxide is adsorbed more strongly than is methane, but only at sites where the electric field strength is sufficiently large. When the introduction of carbon monoxide decreases the peak intensities of preadsorbed methane, it can be assumed that the corresponding sites possess electric fields to some extent. The combination of carbon monoxide and methane also has a geometrical advantage, i.e., their sizes are similar (the Lennard-Jones size parameter σ_{LJ} of methane is 0.3758 nm[7] and that of carbon monoxide is 0.3690 nm[7]). Several groups have used these two probe molecules for the characterization of CeO_2,[8] MgO,[9,10] and zeolite Y.[11] In this study, the usefulness of methane as a probe for basic sites was demonstrated by using microporous titanosilicate ETS-10.

Infrared Absorption Properties of Adsorbed Methane. Methane has four characteristic vibrational frequencies. Among them, the symmetric stretching mode ν_1 and the degenerate deformation mode ν_2 are originally infrared inactive, and they become active when adsorption induces polarization. Since the ν_1 is not complicated by the gas phase and has a higher absorption coefficient than the ν_2, the ν_1 is the most suitable band for this type of characterization. When polarized, the ν_1 shifts to a lower frequency, depending on the degree of polarization. Possible polarizing origins on solid surfaces are acidic sites, basic sites, and strong electric fields. On some kinds of alkali metal ion-exchanged zeolites, such as ZSM-5[12] and zeolite L,[13] the dependencies of the band shifts on the cation radii suggest that the interacting sites are the extraframework cations and the polarizing interactions are mainly electric field-induced dipole interactions. A density functional study of methane interacting with alkali and alkali-earth metal cations[14] also shows that the shifts are proportional to the squares of the electric field strengths. In such cases, the quantitative relationship between a band shift and the strength of the electric field has been estimated by several methods.[1] In the present study, the electric field strengths were calculated by using the quantitative relationship proposed by Duran et al.[15] Although several studies of methane interacting with an electric field have been conducted, there are relatively few reports[8−11] of methane polarized by the basic sites.

Infrared Absorption Properties of Adsorbed Carbon Monoxide. Carbon monoxide has only one stretching mode, and the transition between the ground states of the rotational levels, which causes a Q-branch, is forbidden in the gas phase. However, adsorbed carbon monoxide shows a strong Q-branch, and the band shift relative to the free molecule depends on the configuration and the strength of the interaction between the

* Address correspondence to this author. Phone: +81-3-5841-7348. Fax: +81-3-5800-3806. E-mail: okubo@chemsys.t.u-tokyo.ac.jp.

10.1021/jp027424v CCC: $25.00
Published on Web 07/18/2003

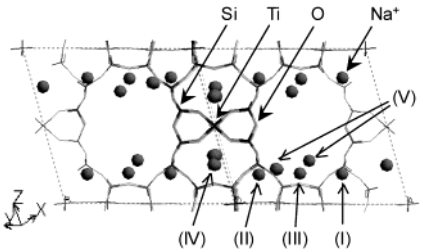

Figure 1. The crystal structure of ETS-10 and the locations of the sodium cations of Na-ETS-10, as proposed by Anderson et al.[22] Sites I−IV are fully occupied, and Site V is randomly occupied with its occupancy adjusted to 0.5.

molecule and the site. Experimental investigations[4,16,17] and computational studies[17−19] of alkali metal ion-exchanged zeolites have shown that carbon monoxide is adsorbed on cationic sites, and the polarizing interaction is an electrostatic interaction. These studies suggest that the band shifts are proportional to the strengths of the electric fields. The quantitative relationship between a band shift and the strength of the electric field has also been calculated by several methods; the results of Pacchioni et al.[19] were used for these calculations in the present study.

In this study, the usefulness of methane was demonstrated by using a crystalline microporous material of ETS-10, with Na- and Cs-exchanged forms. ETS-n is a series of microporous titanosilicates developed by Engelhard Corporation, and the structure of ETS-10 was recently determined by Anderson et al.[20] Strong basicity was reported by Philippou et al. based on selectivity for acetone in 2-propanol conversion reactions.[21] The strong basicity and crystalline nature of this material are advantageous for evaluating the usefulness of methane and methane−carbon monoxide coadsorption in order to characterize basic sites. At the same time, information about the adsorption sites of ETS-10 is useful for the application of ETS-10 itself. The locations of the adsorption sites, as well as the nature and the strength of these sites, are discussed in the present study. For such a discussion, information about the crystal structures and the locations of the cations is necessary. The crystal structures have been resolved with accuracy good enough for the present purposes. However, there are two different models of the cation sites, and the number of accessible sites is not the same. Figure 1 shows the location of the cations at Sites I−V, as proposed by Anderson et al.[22] In this model, there are two accessible sites of Sites III and V in the case of methane. In contrast, in an earlier model suggested by Grillo and Carrazza,[23] Sites I−IV are almost at the same positions as those given in Figure 1, but without Site V. Thus, the Grillo and Carrazza model suggests that there is only one accessible site of Site III. Although our spectra did not support the reliability of these models, the locations of the basic sites were suggested based on our spectroscopic results.

2. Experimental Section

1. Materials. ETS-10 was synthesized by using a seed crystal that was a mixture of ETS-10 and ETS-4. The seed crystal synthesis was performed according to the procedure of Das et al.[24] A diluted titanium tetrachloride solution was prepared by the slow addition of 0.330 mL of pure titanium tetrachloride (99%, Wako) into a vigorously stirred mixture of 1.613 g of hydrochloric acid (35−37%, Wako) and 0.056 g of deionized water, while the mixture was cooled in an ice bath. Sodium hydroxide (0.513 g, Wako) and 2.735 g of deionized water were added under conditions of constant stirring to a mixture of 3.805 g of sodium silicate solution (14% NaOH, 27% SiO_2, Aldrich) and 2.735 g of deionized water. Dropwise addition of the abovementioned titanium tetrachloride solution to the latter mixture under conditions of rapid stirring resulted in a white gel. Then, 0.534 g of potassium fluoride (dehydrated, Wako) was added to the gel, and the mixture was stirred for 1 h. The molar composition of the gel was 8.70 Na:1.89 K:5.69 SiO_2:1.00 Ti:163 H_2O. The gel was transferred to a Teflon-lined autoclave, and the crystallization was carried out at 473 K with a rotation speed of 45 rpm for 16 h. After the crystallization, the product was centrifuged off, washed in water several times, and dried at 353 K overnight.

By using the seed crystal obtained above, the synthesis of ETS-10 was performed according to the procedure of Krishna et al.[25] While being stirred, 3.635 g of sodium silicate solution was mixed with 0.100 g of sodium hydroxide. Then, 0.516 g of potassium fluoride (Wako) and 1.000 g of deionized water were added. To this solution was added slowly 1.465 g of titanium trichloride (24% $TiCl_3$, 7% HCl, Kishida Reagents Chemicals), followed by the addition of 0.288 g of sodium chloride (Wako) and 1.000 g of deionized water. Then, 0.079 g of hydrochloric acid and 0.216 g of deionized water were added to the solution. To the resulting gel were added 0.030 g of the seed crystal and 0.500 g of deionized water. After adding another 1.000 g of water to the final gel, it was stirred for about 1 h. The gel composition was 8.84 Na:3.90 K:7.16 SiO_2:1.00 Ti:168 H_2O. The gel was transferred to an autoclave and heated at 473 K for 5 days. After crystallization, the product was centrifuged off, washed in water several times, and dried at 353 K overnight.

Na and Cs forms of ETS-10 were prepared via ion-exchanges of as-synthesized (Na, K)-ETS-10 with 2 M aqueous solutions of the corresponding alkaline chloride. A mixture of as-synthesized (Na, K)-ETS-10 and the corresponding alkaline chloride solution was stirred at 358 K for about 5 h. The exchange procedure was repeated twice. The final product was washed with deionized water several times and dried at 353 K.

2. Characterization of Materials. The synthesized products were characterized by X-ray diffraction and argon vapor adsorption. The X-ray diffraction patterns were obtained with M03XHF22 (MacScience Co., Ltd) and the argon vapor adsorption measurements were performed with Autosorb-1 (Quantachrome Corp.). In the procedures of argon adsorption, the samples were preheated under a vacuum at 673 K for more than 3 h. The isotherms obtained were analyzed by the *t*-plot method,[26] i.e., by extrapolating the linear portions of the *t*-plots, the micropore volumes were determined. The effective pore diameters were determined by the Saito−Foley method.[27]

3. Infrared Spectroscopy. A variable-temperature cell (Specac Limited) with CaF_2 windows was used for the in situ measurements. The materials were pelletized to 100 μm thick self-standing wafers. The wafers were then preheated at 523 K under vacuum conditions for 3 h, cooled with liquid nitrogen, and then controlled at 113 K with a heater. The adsorbate gases were introduced in the cell in small doses at 113 K. In the subsequent adsorption of carbon monoxide to methane, the carbon monoxide was introduced into the cell without any evacuation of methane. The purity of the methane was 99.9999% and carbon monoxide diluted with helium (1% of carbon monoxide diluted with 99.9999% of helium) was used. Infrared spectra were collected with Magna-IR 560 (Nicolet Instrument Corp.). The resolution was 2 cm^{-1} and the integration was repeated 50 times.

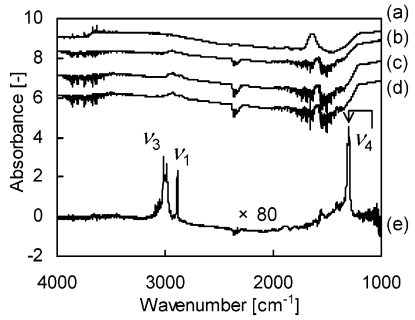

Figure 2. Infrared spectra of Na-ETS-10: (a) as-prepared wafer, (b) after preheating samples at 523 K, (c) after decreasing the temperature to 113 K, (d) after the introduction of methane at 113 K, and (e) difference spectrum of (d)−(c), magnified 80 times along with the vertical axis.

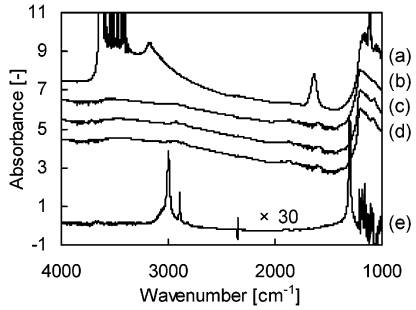

Figure 3. Infrared spectra of Cs-ETS-10: (a) as-prepared wafer, (b) after preheating samples at 523 K, (c) after decreasing the temperature to 113 K, (d) after the introduction of methane at 113 K, and (e) difference spectrum of (d)−(c), magnified 30 times along with the vertical axis.

3. Results and Discussion

1. Characterization of Materials. The X-ray diffraction pattern of the final product was assigned as ETS-10, based on the pattern reported by Anderson et al.,[20] although it contained quartz as a sub-phase. Since such a nonporous phase has a considerably smaller surface area than ETS-10, the existence of quartz is neglected in the following discussion. After the ion-exchange or the heat-treatment at 673 K, the diffraction pattern had hardly changed.

The argon adsorption measurements revealed that the pore volumes of the Na and Cs forms were 0.085 and 0.056 cm^3/g, respectively. The effective pore diameters of both samples were the same at 0.61 nm.

2. Infrared Spectra of Materials. Figures 2 and 3 illustrate the infrared spectra of Na-ETS-10 and Cs-ETS-10, respectively. On both samples, the spectral changes obtained by either preheating or cooling showed similar tendencies. First, the broad bands in the range of 3600−3000 cm^{-1} and the peaks at 1600 cm^{-1} of the as-prepared samples (Figures 2a and 3a) almost disappeared after they had been preheated at 523 K (Figures 2b and 3b). These bands can be assigned as adsorbed water. Then, after the samples had cooled to 113 K (Figures 2c and 3c), no spectral changes were observed.

Figures 2e and 3e show examples of difference spectra of before (Figures 2c and 3c) and after (Figures 2d and 3d) the introduction of methane on Na- and Cs-ETS-10, respectively. Since the difference spectra clearly show the effect of the introduction of gas, they will be used in the remaining discussion.

3. Infrared Spectra of Adsorbed Molecules on Na-ETS-10. Figure 4a shows the spectra of the symmetric stretching mode ν_1 of methane on Na-ETS-10 with increasing equilibrium gas pressure. The spectra clearly revealed that the methane on Na-ETS-10 has two different adsorbed states, in which peaks were observed at 2893 (denoted as "CH_4-middle") and 2885 cm^{-1} (CH_4-low). A peak deconvolution assuming the Gaussian shape for each peak (Figure 4b) indicates the existence of another peak on the side with a higher frequency, 2900 cm^{-1} (CH_4-high). The shift widths $\Delta\nu_1$ of these peaks from the free molecule (2917 cm^{-1} [28]) were −17, −24, and −32 cm^{-1}, beginning from the highest frequency band. These numerical values are summarized in Table 1. In the fourth column of Table 1, the strengths of the electric fields (E) are also listed, if the band was assigned as methane interacting with the electric field (the assignment will be discussed below). For the calculation, the relationship between a band shift ($\Delta\nu_1$) and the electric field strength (E) reported by Duran et al.[15] was employed. Among the three bands, the lowest band (CH_4-low) appeared first, even at the lowest pressure, suggesting that the solid−methane interaction was strongest at the corresponding site.

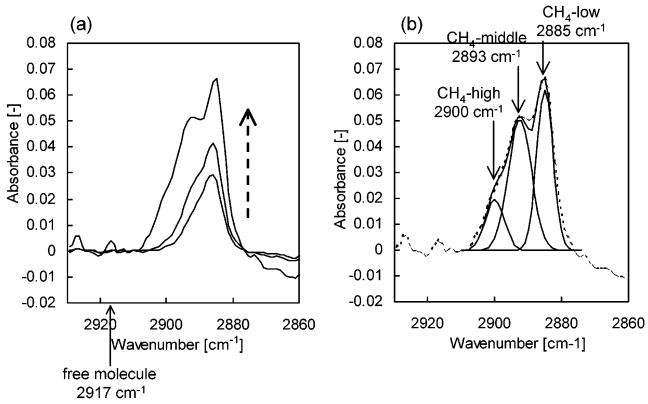

Figure 4. (a) Infrared spectra of methane ν_1 on Na-ETS-10. The dotted arrow indicates an increase in gas-phase equilibrium pressure. (b) Infrared spectra after deconvolution of the highest spectrum of (a).

TABLE 1: The Frequencies (ν_1) and the Shift Widths ($\Delta\nu_1$) of Methane Adsorbed on ETS-10, and the Strengths of the Electric Fields (E) Estimated with the $\Delta\nu_1$ Values

	ν_1 [cm^{-1}]	$\Delta\nu_1$ [cm^{-1}]	E [V/nm][a]
Na-ETS-10			
CH_4-high	2900	−17	
CH_4-middle	2893	−24	9.0
CH_4-low	2885	−32	10.1
Cs-ETS-10	2893	−24	

[a] Estimated according to ref 15.

TABLE 2: The Frequencies (ν) and the Shift Widths ($\Delta\nu$) of Carbon Monoxide Adsorbed on ETS-10, and the Strengths of the Electric Fields (E) Estimated with the $\Delta\nu$ Values

	ν [cm^{-1}]	$\Delta\nu$ [cm^{-1}]	E [V/nm][a]
Na-ETS-10			
CO-high	2176	24	3.9
CO-low	2167	17	2.7
Cs-ETS-10	2145	2	0.32

[a] Estimated according to ref 19.

Figure 5a shows the spectra of adsorbed carbon monoxide on Na-ETS-10, and Figure 5b shows the result of the peak deconvolution. The peak positions (ν) are summarized in Table 2 with the shift widths ($\Delta\nu$) relative to the gas phase ($\nu = 2143$ cm^{-1}, estimated by a gas-phase infrared absorption experiment). The strengths of the electric fields (E) were estimated from the shift widths ($\Delta\nu$) according to the relationship reported by Pacchioni et al.,[19] and these values are also listed in Table 2.

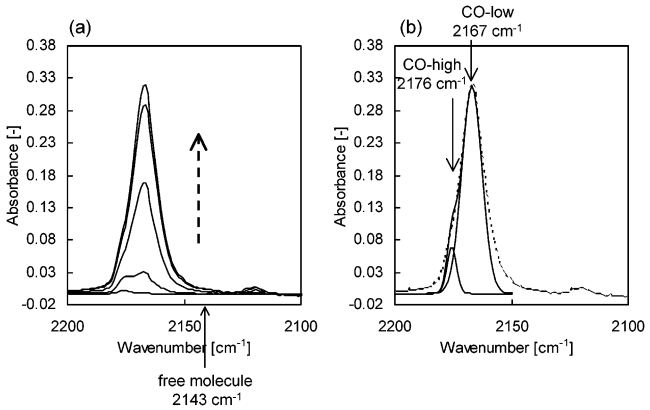

Figure 5. (a) Infrared spectra of carbon monoxide on Na-ETS-10. The dotted arrow indicates the increase of gas-phase equilibrium pressure. (b) Infrared spectra after deconvolution of the highest spectrum of (a).

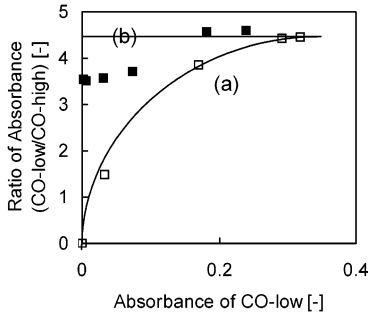

Figure 6. Variations in the intensity ratio of two infrared absorption bands of carbon monoxide (CO-low/CO-high) along with the increase of gas-phase equilibrium pressure of carbon monoxide, which was normalized with the absorption intensity of CO-low. Carbon monoxide was introduced onto (a) fresh Na-ETS-10 and (b) pre-methane-adsorbed Na-ETS-10.

At the lowest gas-phase pressure, only one peak was seen at 2176 cm^{-1} (CO-high); after the gas pressure increased, the main peak was observed at 2167 cm^{-1} (CO-low). The variations in the absorption intensity ratio of these two peaks, along with the increase in equilibrium pressure, are shown in Figure 6a. According to the study of Zecchina et al.,[29] CO-high can be assigned as single carbon monoxide molecules and CO-low can be assigned as complexes of plural molecules adsorbed on one cation. Since the ratio of intensities (CO-low/CO-high) converged to 4.5, and did not diverge to infinity, it is possible that a number of single molecules remained unaffected, even at a high molecular density of the adsorbed phase.

Figure 7 indicates the spectral changes of methane (ν_1) and carbon monoxide by the subsequent adsorption of carbon monoxide to methane on Na-ETS-10. The variations of the absorption intensities are shown in Figure 8a. It is obvious that the peak at the highest frequency of methane (CH_4-high) was not affected by carbon monoxide. Since methane molecules interacting with strong electric fields are thought to be replaced by carbon monoxide molecules, this unaffected peak was assigned as a methane molecule interacting with something other than an electric field, e.g., possibly a framework oxygen atom acting as a basic site. In contrast, the peaks of CH_4-low and CH_4-middle decreased after the introduction of carbon monoxide. As mentioned in the Introduction, several studies[4,15−18] of alkali metal ion-exchanged zeolites have indicated that carbon monoxide interacts with the extraframework cations. Thus, it can be concluded that methane molecules corresponding to these two peaks are replaced by carbon monoxide molecules which were adsorbed on the cationic sites (see Figures 7c and 9a). However, this conclusion does not necessarily mean that the methane molecules had been adsorbed only on the cationic sites. For the interpretation of the spectral changes, an interaction with framework oxygen atoms (Figure 9b) should also be considered. Moreover, there is some possibility of an indirect exclusion of methane by carbon monoxide (Figure 9c). Thus, it remains difficult to propose the most appropriate model. The determination of the symmetry of the configuration renders it possible to discuss the validity of these models. The symmetry of adsorbed methane is related to the infrared activity of the ν_1 and ν_2 modes, and also to the number of absorption bands of ν_2, ν_3, and ν_4[2]; if the configuration shows C_{3v} symmetry, then ν_2 shows one band, and ν_3 and ν_4 show 2 bands each. In the case of C_{2v} and C_1 symmetry, ν_2 shows two bands, and ν_3 and ν_4 show 3 bands each. Since the ν_1 mode became infrared active, it can be concluded that the symmetry of the configuration of methane was C_{3v} or lower. However, as the absorption intensity of the ν_2 mode was too small to detect, and the spectra of the ν_3 and ν_4 bands were too complicated to accurately determine the number of bands, it was not possible to offer a more detailed discussion for these cases. The determination of the exact locations of the cations will be helpful for further discussion.

The variation of the ratio of the peak intensities (CO-low/CO-high) is shown together with the increase in carbon monoxide pressure in Figure 6b. When methane was already adsorbed on Na-ETS-10, the ratio remained constant at 4.5 during the process. This result also suggests that some individual

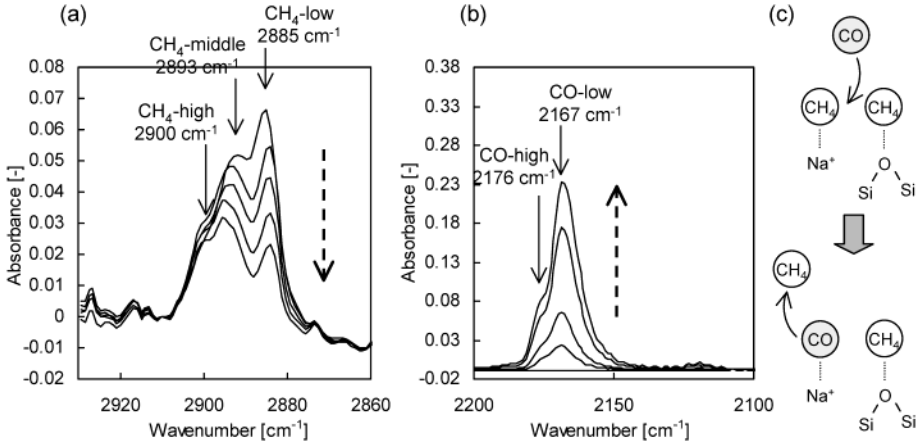

Figure 7. Spectral changes of (a) methane ν_1 and (b) carbon monoxide along with the subsequent adsorption of carbon monoxide to methane on Na-ETS-10. The dotted arrows indicate an increase in the gas-phase equilibrium pressure of carbon monoxide. (c) Image of the replacement of methane by carbon monoxide on cationic sites.

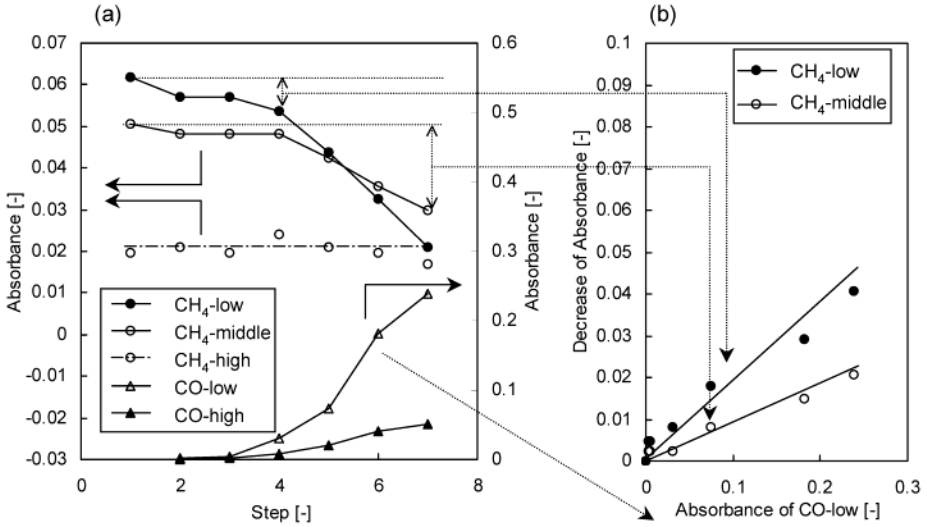

Figure 8. (a) Variations of the absorption intensity of methane and carbon monoxide along with the increase in the gas-phase equilibrium pressure of carbon monoxide. The larger the step, the higher the equilibrium pressure. (b) Dependencies of the decrease in CH_4-middle and CH_4-low on the intensity of CO-low.

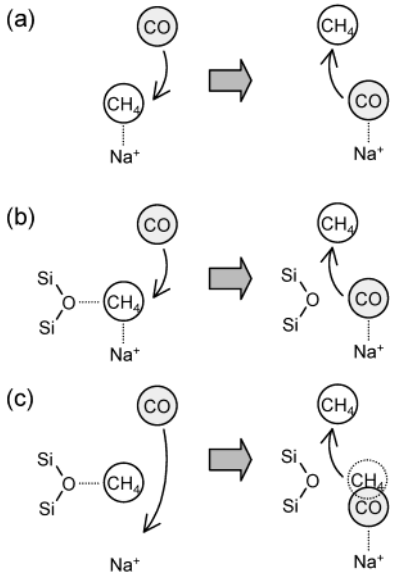

Figure 9. Possible explanations of adsorption sites for CH_4-middle and CH_4-low.

molecules remained unaffected, even with an adsorbed phase of high molecular density.

The increase in CO-low and the decreases in CH_4-low and CH_4-middle revealed a linear relationship, as shown in Figure 8b. As the ratio of CO-low/CO-high was almost constant, these two peaks for methane also showed a similar linearity with that of CO-high. This finding suggests that methane molecules were replaced by carbon monoxide molecules at the corresponding sites.

4. Infrared Spectra of Adsorbed Molecules on Cs-ETS-10. In the case of Cs-ETS-10 (Figure 10), adsorbed methane showed only one peak at 2893 cm^{-1}. Adsorbed carbon monoxide also showed a single absorption band at 2145 cm^{-1}, as shown in Figure 11. Those values are summarized in Tables 1 and 2 with the shift width ($\Delta\nu$) relative to the free molecule. Compared with the results obtained with Na-ETS-10, the small shift width ($\Delta\nu = 2$ cm^{-1}) of carbon monoxide on Cs-ETS-10 indicates that the electric field in the pore of Cs-ETS-10 was extremely weak. In contrast, the adsorbed methane showed a relatively large shift ($|\Delta\nu_1| = 24$ cm^{-1}) when compared even

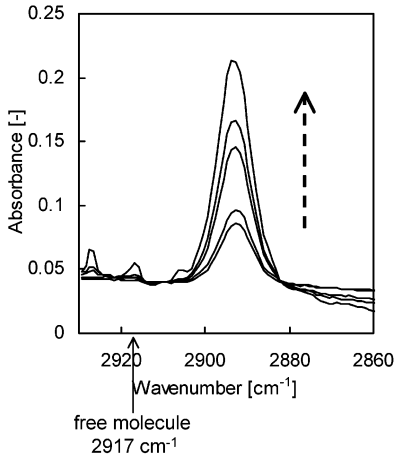

Figure 10. Infrared spectra of methane ν_1 on Cs-ETS-10. The dotted arrow indicates an increase in gas-phase equilibrium pressure.

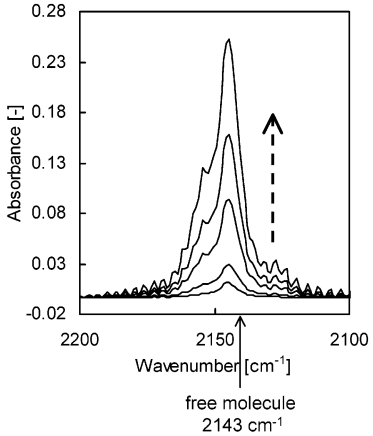

Figure 11. Infrared spectra of carbon monoxide on Cs-ETS-10. The dotted arrow indicates an increase in gas-phase equilibrium pressure.

with the largest shift ($|\Delta\nu_1| = 32$ cm^{-1}) of CH_4-low on Na-ETS-10. This finding indicates that the methane was polarized by some interaction other than that with an electric field. A framework oxygen atom acting as a basic site could be considered as an origin of this interaction.

5. Relationship with Catalytic Performance. Philippou et al. reported that the acetone selectivity from 2-propanol was

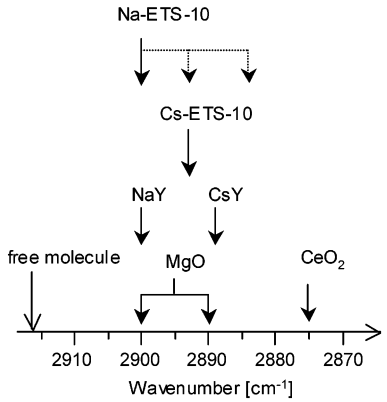

Figure 12. Frequencies of absorption bands of methane ν_1 which were assigned as methane molecules adsorbed on basic sites, on ETS-10, CeO_2,[8] MgO,[9] and zeolite Y.[11] The dotted arrows of Na-ETS-10 indicate the bands with some possibility of being basic sites.

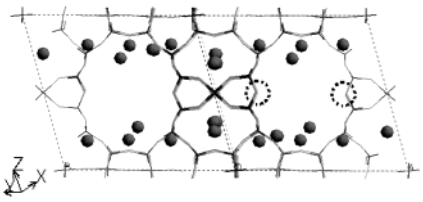

Figure 13. Possible locations (dotted circles) of basic sites of Na-ETS-10.

higher on Cs-ETS-10 than on as-synthesized (Na, K)-ETS-10, and they concluded that the basicity of the former is stronger.[21] Three infrared absorption bands appeared; these bands can be considered to be basic sites on Na-ETS-10. Thus, the comparison of basicity between these materials was not straightforward. The present results revealed the existence of a strong electric field of cationic sites on Na-ETS-10, which could act as a Lewis acid. The coexistence of Lewis acidic sites would lead to a decrease in the acetone selectivity on Na-ETS-10 relative to that on Cs-ETS-10.

The infrared absorption bands of methane, which was thought to be interacting with basic sites, are illustrated in Figure 12, together with several frequency values reported in association with other materials.[8,9,11] The strengths of the basic sites of Na-ETS-10 and Cs-ETS-10 are in the same order with those of MgO,[9] NaY,[11] and CsY.[11]

6. Location of the Adsorption Sites. In addition to information about the nature and the strength of active sites, infrared spectroscopy provides useful information about site locations. Our results on Na-ETS-10 showed the existence of a basic site that was not affected by the coexistence of carbon monoxide (CH_4-high of Figure 7a, see also Figure 8a). This finding indicates that at least one single basic site is far from each cation. For such sites, candidate framework oxygen atoms are indicated in Figure 13. Taking molecular size into consideration, a methane molecule could potentially be adsorbed on these basic oxygen atoms, even when all of the nearest cationic sites were occupied by carbon monoxide molecules.

In the case of Cs-ETS-10, methane showed only one absorption band; therefore, it is difficult to come to conclusions about the site location. However, it would be reasonable to consider the same oxygen atoms as those occurring in Na-ETS-10 as candidates.

4. Conclusions

In this study, the usefulness of methane as a probe for basic sites was demonstrated. In the case of Na-ETS-10, methane showed three adsorption bands in the region of the symmetric stretching mode ν_1. One of these bands, i.e., the one located at 2900 cm^{-1}, was considered as methane adsorbed on a basic site, since it was not affected by carbon monoxide. On the other hand, there remain three possible explanations for the other two bands at 2893 and 2885 cm^{-1}. In the case of Cs-ETS-10, there appeared only one absorption band of ν_1 at 2893 cm^{-1}. Since the electric field estimated from the shift width ($\Delta\nu$) of carbon monoxide was extremely small, the band of methane at 2893 cm^{-1} could be assigned as methane adsorbed on a basic site. From the frequencies of these bands, the basicities of Na- and Cs-ETS-10 were estimated to be in the same degree with those of other basic materials such as MgO, NaY, and CsY. Since one of the absorption bands of methane at 2900 cm^{-1} on Na-ETS-10 was not replaced by carbon monoxide, it was revealed that at least one kind of basic site is located far from each cation. On the basis of this fact, the locations of basic framework oxygen atoms were proposed.

Acknowledgment. This study was financially supported by the Research Institute of Innovative Technology for the Earth (RITE) and Nissan Science Foundation. We are grateful to Prof. Tatsuya Yamazaki of Ishinomaki Senshu University for his helpful advice, in particular regarding the sample wafer preparation. We also wish to thank Dr. Masaru Ogura for fruitful discussions and Mr. Hirotaka Mizuhata for his contribution to the material synthesis.

References and Notes

(1) Bishop, D. M. *J. Chem. Phys.* **1993**, *98*, 3179.

(2) Knözinger, H. *Handbook of Heterogeneous Catalysis*; Ertl, G., Knözinger, H., Wetkamp, J., Eds.; Wiley-VCH: Weinheim, Germany, 1997; Vol. 2, p 707.

(3) Lavalley, J. C. *Catal. Today* **1996**, *27*, 377.

(4) Knözinger, H.; Huber, S. *J. Chem. Soc., Faraday Trans.* **1997**, *94*, 2047.

(5) Bosch, E.; Huber, S.; Weitkamp, J.; Knözinger, H. *Phys. Chem. Chem. Phys.* **1999**, *1*, 579.

(6) Sánchez-Sánchez, M.; Blasco, T.; Rey, F. *Phys. Chem. Chem. Phys.* **1999**, *1*, 4529.

(7) Reid, R. C.; Prausnitz, J. M.; Ploing, J. E. *The Properties of Gases and Liquids*, 4th ed.; McGraw-Hill: New York, 1987.

(8) Li, C.; Xin, Q. *J. Phys. Chem.* **1992**, *96*, 7714.

(9) Li, C.; Li, G.; Xin, Q. *J. Phys. Chem.* **1994**, *98*, 1993.

(10) Ferrari, A. M.; Huber, S.; Knözinger, H.; Neyman, K. M.; Rösch, N. *J. Phys. Chem. B* **1998**, *102*, 4548.

(11) Huber, S.; Knözinger, H. *Chem. Phys. Lett.* **1995**, *244*, 111.

(12) Yamazaki, T.; Watanuki, I.; Ozawa, S.; Ogino, Y. *Langmuir* **1988**, *4*, 433.

(13) Yamazaki, T.; Honma, K.; Katoh, M.; Ozawa, S. *Chem. Lett.* **1996**, 1101.

(14) Ferrari, A. M.; Neyman, K. M.; Huber, S.; Knözinger, H.; Rosch, N. *Langmuir* **1998**, *14*, 5559.

(15) Duran, M.; Andrés, J. L.; Lledós, A.; Bertrán, J. *J. Chem. Phys.* **1989**, *90*, 328.

(16) Zecchina, A.; Bordiga, S.; Lamberti, C.; Spoto, G.; Carnelli, L.; Areán, C. O. *J. Phys. Chem.* **1994**, *98*, 9577.

(17) Ugliengo, P.; Garrone, E.; Ferrari, A. M.; Zecchina, A.; Arean, C. O. *J. Phys. Chem. B* **1999**, *103*, 4839.

(18) Ferrari, A. M.; Ugliengo, P.; Garrone, E. *J. Chem. Phys.* **1996**, *105*, 4129.

(19) Pacchioni, G.; Cogliandro, G.; Bagus, P. S. *Int. J. Quantum Chem.* **1992**, *42*, 1115.

(20) Anderson, M. W.; Terasaki, O.; Ohsuna, T.; Philippou, A.; MacKay, S. P.; Ferreira, A.; Rocha, J.; Lidin, S. *Nature* **1994**, *367*, 347.

(21) Philippou, A.; Rocha, J.; Anderson, M. W. *Catal. Lett.* **1999**, *57*, 151.

(22) Anderson, M. W.; Agger, J. R.; Luigi, D.-P.; Baggaley, A. K.; Rocha, J. *Phys. Chem. Chem. Phys.* **1999**, *1*, 2287.

(23) Grillo, M. E.; Carrazza, J. *J. Phys. Chem.* **1996**, *100*, 12261.

(24) Das, T. K.; Chandwadkar, A. J.; Sivasanker, S. *Chem. Commun.* **1996**, 1105.
(25) Krishna, R. M.; Prakash, A. M.; Kurshev, V.; Kevan, L. *Phys. Chem. Chem. Phys.* **1999**, *1*, 4119.
(26) Lippens, B. C.; Linsen, B. G.; de Boer, J. H. *J. Catal.* **1964**, *3*, 32.
(27) Saito, A.; Foley, H. *AIChE J.* **1991**, *37*, 429.
(28) Nakamoto, K. *Infrared and Raman Spectra of Inorganic and Coordination Compounds*, 4th ed.; John Wiley & Sons: New York, 1986; Vol. 2.
(29) Zecchina, A.; Arean, C. O.; Palomino, G. T.; Geobaldo, F.; Lamberti, C.; Spoto, G.; Bordiga, S. *Phys. Chem. Chem. Phys.* **1999**, *1*, 1649.